

# Title: The Role of Vitamin D in *Emiliania huxleyi*: A Microalgal Perspective on UV-B Exposure

**Authors:** Or Eliason<sup>1</sup>, Sergey Malitsky<sup>2</sup>, Irina Panizel<sup>2</sup>, Ester Feldmesser<sup>2</sup>, Martin Sperfeld<sup>1</sup>, Einat Segev<sup>1\*</sup>

## Affiliations:

<sup>1</sup>Department of Plant and Environmental Sciences, Weizmann Institute of Science; Rehovot, 7610001, Israel.

<sup>2</sup>Department of Life Sciences Core Facilities, Weizmann Institute of Science; Rehovot, 7610001, Israel.

\*Corresponding author. Email: Einat.Segev@weizmann.ac.il

## Abstract

An essential interaction between sunlight and eukaryotes involves the production of vitamin D through exposure to ultraviolet-B (UV-B) radiation. While extensively studied in vertebrates, the role of vitamin D in non-animal eukaryotes like microalgae remains unclear. *Emiliania huxleyi*, a microalga inhabiting shallow ocean depths exposed to UV-B radiation, is well-suited for this research. Our results show that *E. huxleyi* can produce vitamin D<sub>2</sub> and D<sub>3</sub>, pointing to their potential role in the algal physiology. We further show that *E. huxleyi* algae respond to vitamin D at the transcriptional level, regulating the expression of protective mechanisms such as the light-harvesting complex stress-related protein (LHCSR) and heme oxygenase, and that vitamin D enhances the algal photosynthetic performance while reducing harmful reactive oxygen species buildup. Understanding the function of vitamin D in *E. huxleyi* has broader implications, shedding light on its role in non-animal eukaryotes and its potential importance in marine ecosystems. This research sets the stage for further investigations into the complex relationship between sunlight, vitamin D, and microalgal physiology, which contributes to our understanding of how eukaryotes adapt to diverse environmental conditions.

29 **Introduction**

30 Life on Earth has a complex relationship with sunlight, relying on its energy for certain processes  
31 while simultaneously requiring protection against its potential harmful effects. A molecular  
32 process that is tightly linked to sunlight is the formation of vitamin D following exposure to  
33 ultraviolet-B (UV-B) radiation emitted from the sun. Vitamin D (calciferol) comprises a group of  
34 steroids that result from the photochemical transformation of several sterol precursors by UV-B  
35 wavelengths<sup>1</sup>. The most common vitamin D species known to occur naturally are vitamin D<sub>2</sub> and  
36 D<sub>3</sub>, originating from the conversion of ergosterol and 7-dehydrocholesterol, respectively<sup>2,3</sup>.

37 In mammals and other studied vertebrates, vitamin D functions as a hormone, involved in the  
38 regulation of a multitude of intracellular and physiological processes vital for the organism  
39 survival and well-being<sup>4</sup>. Vitamin D is pivotal in facilitating the absorption and homeostasis of  
40 essential ions such as Ca<sup>2+</sup> and PO<sub>4</sub><sup>3-</sup><sup>5,6</sup>, and vitamin D deficiency has been linked to a range  
41 of physiological disorders<sup>7,8</sup>. Due to its key role in human health, vitamin D has been the focus  
42 of biological and pharmaceutical research endeavors. These efforts have been directed towards  
43 understanding the mechanisms through which it operates in humans and human models.

44 However, mounting evidence suggests that vitamin D has been a constituent of eukaryotes long  
45 before the emergence of vertebrates. This is evident not only in the identification of vitamin D in  
46 distant eukaryotic lineages like algae<sup>9-11</sup>, plants<sup>12</sup>, and fungi<sup>13-15</sup> but also in the preservation of  
47 vitamin D-related biomarkers, likely from an algal source, in marine sediments dating back over  
48 600 million years<sup>16</sup>.

49 Despite its widespread presence across diverse lineages, our understanding of the physiological  
50 role of vitamin D in non-animal eukaryotes remains limited. Non-animal eukaryotes, namely  
51 microalgae, have been suggested as potential sources of vitamin D for higher trophic levels in  
52 the marine environment<sup>17-19</sup>. But the processes underlying vitamin D production and regulation  
53 in microalgae remain largely unexplored<sup>20</sup>.

54 While UV-B radiation is crucial for vertebrate health due to its role in vitamin D formation, it can  
55 also be detrimental, causing direct damage to biomolecules like DNA, leading to the generation  
56 of reactive oxygen species (ROS)<sup>21-23</sup>, and can ultimately result in cell death<sup>24</sup>. Photosynthetic  
57 organisms, like algae, are particularly susceptible to UV-B damage, as their energy production

58 hinges on exposure to solar radiation<sup>25,26</sup>. Although water acts as a UV-B filter<sup>27</sup>, significant  
59 intensities can still penetrate the upper layers of ocean surfaces<sup>28</sup>, potentially impacting  
60 organisms such as algae<sup>29</sup>.

61 Microalgae of the species *Emiliania huxleyi*, also named *Gephyrocapsa huxleyi*<sup>30</sup>, are widely  
62 distributed in modern oceans and play key roles in various biogeochemical cycles<sup>31,32</sup>. These  
63 algae are known to flourish in high light environments at shallow depths of about 10 to 20  
64 meters<sup>33</sup>, where exposure to UV-B wavelengths is likely. Earlier findings provided intermittent  
65 indications that *E. huxleyi* algae might possess the inherent capability to synthesize vitamin D.  
66 These reports highlighted the algal capacity to generate vitamin D<sub>2</sub> upon exposure to UV-B  
67 irradiation<sup>11</sup>, its cholesterol content<sup>34,35</sup>, and the presence of a gene analogous to 7-  
68 dehydrocholesterol reductase (DHCR7) responsible for converting 7-dehydrocholesterol into  
69 cholesterol<sup>36</sup>.

70 In this study we explore the overlooked role of vitamin D in *E. huxleyi*. Specifically, we investigate  
71 the relationship between vitamin D formation following exposure to UV-B and the regulation of  
72 cellular mechanisms that operate in response to harmful radiation.

73

## 74 **Results**

### 75 *E. huxleyi* algae produce vitamin D<sub>2</sub> and D<sub>3</sub>

76 To investigate whether vitamin D species are formed by *E. huxleyi* algae upon exposure to UV,  
77 we cultivated algal cultures in a chamber with environmentally relevant UV-B radiation levels  
78 (see Materials and Methods). Metabolic analyses revealed the presence of both D<sub>2</sub> and D<sub>3</sub> in  
79 these algal cultures (Table 1). Our results show that D<sub>2</sub> was significantly enriched in UV-exposed  
80 cultures, with levels of approximately ~4 ng/mg dry weight, while it was barely detected in  
81 cultures that were not exposed to UV. The D<sub>2</sub> precursor ergosterol was found in both UV-treated  
82 and control cultures. Lower amounts of vitamin D<sub>3</sub> (~0.04 ng/mg dry weight) were detected in  
83 both UV-treated and control cultures.

84 Importantly, while D<sub>2</sub> detection was consistent across all analyzed UV-exposed samples, D<sub>3</sub> was  
85 identified only in part of the experiments during our research. Interestingly, when D<sub>3</sub> was  
86 detected, its precursor 7-dehydrocholesterol, was detected as well. Inconsistent detection of D<sub>3</sub>

87 was previously reported in plants, and was attributed to the sensitivity of the analytical method  
88 used<sup>37</sup>. Our many efforts to resolve the variable measurements of D<sub>3</sub> were not successful (see  
89 detailed description of attempts in Materials and Methods). Collectively, our findings  
90 demonstrate that *E. huxleyi* algae produce D<sub>2</sub> and D<sub>3</sub>, suggesting a possible cellular function for  
91 vitamin D.

92 *E. huxleyi* algae show a transcriptomic response to UV radiation

93 UV radiation is necessary for the formation of vitamin D<sup>2</sup>. Therefore, we sought to explore the  
94 transcriptomic response of *E. huxleyi* algae to UV exposure, aiming to elucidate cellular  
95 processes that may be related to vitamin D. To achieve this, we analyzed the *E. huxleyi*  
96 transcriptome using cultures that were grown under continuous UV exposure during the light  
97 period of the daily light/dark cycle, in comparison to algal cultures that were protected from the  
98 UV source. Cultures were sampled for RNA-sequencing at three time points representing  
99 different growth phases (days 7, 10, and 13, see Fig. S1).

100 The transcriptomic analysis revealed differential expression (DE) of 374 genes between UV-  
101 exposed and control cultures (Table S1). Of these genes, 172 were annotated with GO terms  
102 related to a known function or process. The annotated genes that were DE in the transcriptome  
103 under UV exposure were associated with various cellular processes including intracellular  
104 signaling pathways and stress response mechanisms. Notably, genes participating in the inositol

Compound	UV (ng / mg)	Control (ng / mg)
D <sub>2</sub>	4.32 ± 1.39 *	0.09 ± 0.01
D <sub>3</sub>	0.038 ± 0.001	0.039 ± 0.001
Ergosterol	83.01 ± 28.96	71.76 ± 9.53
7-dehydrocholesterol	0.24 ± 0.04 *	0.16 ± 0.02

**Table 1. *E. huxleyi* algae produce vitamin D<sub>2</sub> and D<sub>3</sub>.** Metabolic analysis of vitamin D species and precursors under UV and control conditions, using algal cultures at day 10 of growth. Values are of ng / mg dry weight. Statistically significant differences ( $P < 0.05$ ) between treatments are marked by \*, calculated using two-sample t-test assuming equal variances. ± values indicate standard deviation based on 4 biological replicates.

105 3-phosphate/calcium ( $IP_3/Ca^{2+}$ ) and the oxylipin signaling pathways were DE (Table 2), both  
106 playing key roles in stress response mechanisms across different organisms<sup>38–42</sup>.

107 Furthermore, a substantial number of DE genes were involved in various stress responses,  
108 including DNA damage sensing and repair, oxidative stress mitigation, protective pigment  
109 biosynthesis, and maintenance of the photosynthetic machinery. Interestingly, several of the  
110 genes and pathways that were DE in *E. huxleyi* algae, are known to be associated with UV  
111 exposure and vitamin D biosynthesis in vertebrates. For instance, the  $IP_3/Ca^{2+}$  and  
112 prostaglandins pathways are involved in UV stress response in mammals<sup>43,44</sup>, and vitamin D is  
113 involved in the regulation of these pathways<sup>45–49</sup>. In mammals, vitamin D also plays a role in  
114 oxidative stress mitigation, DNA repair, and the regulation of various enzymes related to stress  
115 response including heme oxygenase, glutathione peroxidase, and tyrosinase<sup>50–54</sup>. Considering  
116 the role of vitamin D in regulating stress response mechanisms in mammals, and the presence  
117 of similar mechanisms regulated by UV in *E. huxleyi*, it seems plausible that vitamin D plays a  
118 role in regulating the algal stress responses.

119 To further explore the observed transcriptomic response induced by UV using an independent  
120 approach, several genes that were regulated in the algal transcriptome were analyzed by qRT-  
121 PCR. RNA was extracted from cultures that were exposed to UV for a duration of 1 hour at day  
122 10 of growth (Fig. 1, S2). Under these conditions, the investigated genes showed significant  
123 upregulation. The differences observed between the two transcriptomic assays, could be the  
124 result of a different response elicited by a prolonged compared to a brief UV exposure.

#### 125 Vitamin D upregulates expression of UV-regulated genes

126 Next, we explored whether vitamin D is indeed involved in regulating stress response  
127 mechanisms in *E. huxleyi* under UV. If vitamin D is synthesized upon UV exposure and plays a  
128 role in regulating the algal stress response to UV, external addition of vitamin D could potentially  
129 induce algae to react as if they were exposed to UV. Therefore, we

130

Gene ID	Putative protein or domain	Differential expression			Protein function
Genes related to intracellular signaling		d. 7	d. 10	d. 13	
G10384	Lipoxygenase domain	-0.46	-1.27	2.04	Oxylipin biosynthesis
G14992	Prostaglandin F(2-alpha) synthase	0.38	0.22	1.75	Oxylipin biosynthesis
G12340	Cytosolic phospholipase A2 domain	-0.51	-0.82	1.70	Oxylipin biosynthesis; Intracellular signaling
G14502	Ca-binding domain	-0.57	-1.12	1.67	Shares similarity to <i>A. thaliana</i> calmodulin-like protein; Intracellular signaling.
G21784	Phosphoinositide phospholipase C	-0.52	-0.62	1.50	IP <sub>3</sub> signaling initiation; cytosolic calcium regulation
G15496	Phosphoinositide 5-phosphatase	0.54	0.74	1.46	IP <sub>3</sub> signaling; cytosolic calcium regulation
G25467	Steroid hydroxylase	1.15	1.49	1.16	Shares similarity to rat <i>cyp1a2</i> with a suggested 25-cholesterol hydroxylase activity
G1648	Mannosyl phosphorylinositol ceramide synthase	-0.37	-0.21	0.98	Potentially involved in Calcium signaling
G19702	Phosphatidylinositol 3-kinase	-0.17	0.00	0.95	IP <sub>3</sub> signaling
G27192	Calcineurin B-like interacting protein kinase	-0.34	1.25	-0.3	Involved in Ca-mediated signaling; Abiotic stress response
Genes related to stress response					
G27084	Deoxyribodipyrimidine photolyase	0.93	1.9	4.29	UV-damage DNA repair
G647	3-dehydroquinate synthase domain	-0.31	5.33	4.07	Shikimate pathway; potentially involved in the production of UV-protective compounds
G22973	Sirtuin 2	1.16	0.89	1.49	DNA transcription and repair
G16746	Tyrosinase Cu-binding domain	-0.54	-1.09	1.46	Involved in synthesis of protective pigments and antioxidants
G18590	Light-harvesting protein	0.51	1.22	1.13	Shares similarity to <i>C. reinhardtii</i> LHCSR; Alleviates photo-oxidative stress
G12503	Poly ADP-ribose polymerase Zn-finger domain	0.62	1.13	1.08	DNA damage sensor
G18115	Deoxyribodipyrimidine photolyase	0.24	0.25	0.99	UV-damage DNA repair
G6690	Glutathione peroxidase	0.05	0.32	0.98	Oxidative stress mitigation
G25108	Chalcone synthase 2	-0.36	-0.43	0.82	Potentially involved in UV protection
G2876	DNA-(apurinic or apyrimidinic site) lyase	0.56	0.52	0.81	DNA repair
G26038	ATP-dependent DNA helicase	-0.34	-0.76	0.79	DNA stability and repair
G8907	(6-4)DNA photolyase	0.07	0.43	0.78	UV-damage DNA repair
G2511	Heme oxygenase	0.37	0.96	0.67	Oxidative stress mitigation
G16133	Formamidopyrimidine-DNA glycosylase	0.49	0.89	0.53	DNA repair
G832	Protochlorophyllide reductase	1.23	-0.41	0.2	Chlorophyll biosynthesis
G22197	5'-tyrosyl DNA phosphodiesterase	0.83	0.22	0.10	DNA repair

**Table 2. Differential expression (DE) of genes associated with signaling and stress response mechanisms in *E. huxleyi* that were upregulated under UV.** DE values calculated according to the transcriptomic analysis are given for days 7, 10 and 13 of growth (designated d. 7, d. 10 and d. 13). Genes are ordered according to DE values at day 13. Full DE and NCBI accession data is presented in Table S1 and Data S1.

131 supplemented algal cultures with vitamin D and monitored the expression of stress response-  
132 related genes via qRT-PCR.

133 Algal cultures were treated with D<sub>2</sub>, D<sub>3</sub>, or with a combination of both, as this combination had a  
134 synergistic impact on algal growth compared to each species alone (Fig. S2). Control cultures  
135 were not treated with vitamin D and were exposed to either normal growth conditions or to UV  
136 radiation for 1 hour. RNA was collected from all cultures 1 hour post treatment.

137 Our analyses revealed four genes that exhibit upregulated expression both upon vitamin D  
138 treatment and UV radiation (Fig. 1). The upregulation of these genes by UV was observed also  
139 in the transcriptomic analysis (Tables 2, S1). Notably, in vitamin D-treated cultures, the  
140 upregulation was only observed following the addition of both D<sub>2</sub> and D<sub>3</sub>. The four upregulated  
141 genes encode for light-harvesting complex stress-related protein (LHCSR, G18590), heme  
142 oxygenase (G2511), steroid hydroxylase (G25467), and a Ca-binding protein (G26534). Both  
143 LHCSR and heme oxygenase are proteins related to the algal stress response.

144 The LHCSR gene is known to exhibit increased expression in moss and green algae under UV-  
145 B and high-light stress, promoting excess energy dissipation in the light-harvesting complex and  
146 thereby reducing photo-oxidative stress<sup>55-57</sup>. Heme oxygenases are enzymes involved in the  
147 formation of antioxidants in plants and animals, with known upregulated expression in response  
148 to UV-B and other ROS-forming stressors<sup>58-60</sup>. UV-B radiation is a fundamental component of  
149 high-light environments, and vitamin D is produced under UV-B radiation (Table 1) and triggers  
150 the upregulation of oxidative- and photooxidative-stress mitigation pathways. Therefore, it is  
151 likely that vitamin D is part of a cellular signaling cascade that reports on and reacts to harmful  
152 light intensities or radiation.

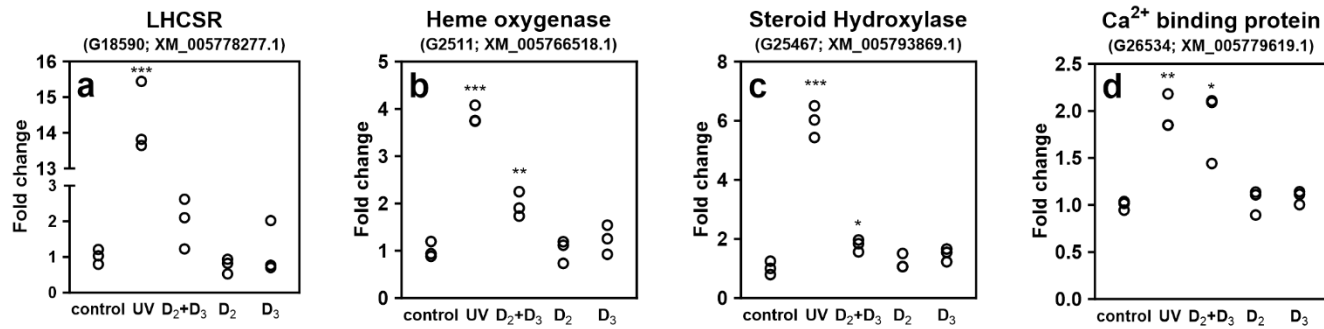


**Figure 1. Combined treatment of vitamin D<sub>2</sub> and D<sub>3</sub> upregulates UV-responsive genes.** qRT-PCR analysis of genes following 1 hour of UV exposure or vitamin D treatments. Top title denotes gene products. In brackets: gene identifier in *E. huxleyi* CCMP3266<sup>94</sup> and matching gene transcript in the *E. huxleyi* CCMP1516 reference genome<sup>95</sup>. Statistical significance compared to control was calculated using two-tailed t-test assuming equal variances. One, two or three asterisks indicate P < 0.05, P < 0.01 and P < 0.001, respectively.

153 Vitamin D treatment improves the algal photosynthetic performance following excess light

154 To investigate the involvement of vitamin D in the cellular response towards harmful light  
155 intensities, we tested the impact of vitamin D treatment on algal physiology, namely  
156 photosynthetic performance, under excess light. To this end, algal cultures were exposed to low,  
157 non-saturating light levels that are regularly used during incubation<sup>61</sup> (130 µmol photons m<sup>-2</sup> s<sup>-1</sup>,  
158 or PAR), and to saturating light<sup>62</sup> (1000 PAR) for 2 hours. Algal cultures under each light regime  
159 were either treated with both D<sub>2</sub> and D<sub>3</sub>, or not treated as control. Algal photosynthetic  
160 performance was evaluated by measuring nonphotochemical chlorophyll fluorescence  
161 quenching (NPQ) as a proxy for the ability of algae to dissipate excess absorbed light energy  
162 into heat<sup>63</sup>. In addition, the maximum PSII quantum yield (F<sub>v</sub>/F<sub>m</sub>) was measured as an indicator  
163 of photosynthetic efficiency<sup>64</sup>. Our results showed that algae under saturating light display  
164 decreased NPQ and F<sub>v</sub>/F<sub>m</sub>, indicative of photoinhibition<sup>61</sup> (Fig. 2a, b). Furthermore, vitamin D-  
165 treated cultures exhibited significantly higher NPQ following exposure to excess light (Fig. 2a,  
166 S4), in comparison to untreated cultures. The cultures that were treated with vitamin D also  
167 demonstrated enhanced F<sub>v</sub>/F<sub>m</sub> (Fig. 2b). These findings emphasize the potentially central role  
168 of vitamin D in algal physiology under harmful light levels. Vitamin D appears to activate cellular  
169

170 processes that enhance excess light energy dissipation  
171 and improve photosynthetic quantum yields.

172 Vitamin D alleviates ROS accumulation under excess  
173 light

174 Under excess light, photosynthetic organisms are likely  
175 to experience oxidative stress<sup>65</sup>, and NPQ is a key  
176 process in mitigating oxidative stress induced by  
177 excess light. Our analyses revealed elevated NPQ in  
178 vitamin D-treated cultures following excess light.  
179 Therefore, we assessed whether addition of vitamin D  
180 to algal cultures under excess light, indeed alleviates  
181 oxidative stress resulting in decreased cellular levels of  
182 ROS. To achieve this, we subjected algal cultures to  
183 excess light (1000 PAR) and assessed the intracellular  
184 ROS levels using the cell-permeable fluorescent probe  
185 2,7-Dichlorodihydrofluorescein diacetate (H<sub>2</sub>DCF-DA).  
186 The tested algal cultures were either treated with both  
187 D<sub>2</sub> and D<sub>3</sub> or were untreated. Additionally, control  
188 cultures were exposed to regular light intensities (130  
189 PAR) and subjected to the same treatments. Our  
190 findings revealed a substantial decrease in intracellular  
191 ROS levels in algae that were treated with vitamin D  
192 and exposed to excess light, compared with untreated  
193 algae under the same light regime (Fig. 2c). These  
194 findings further support a cellular role of vitamin D in

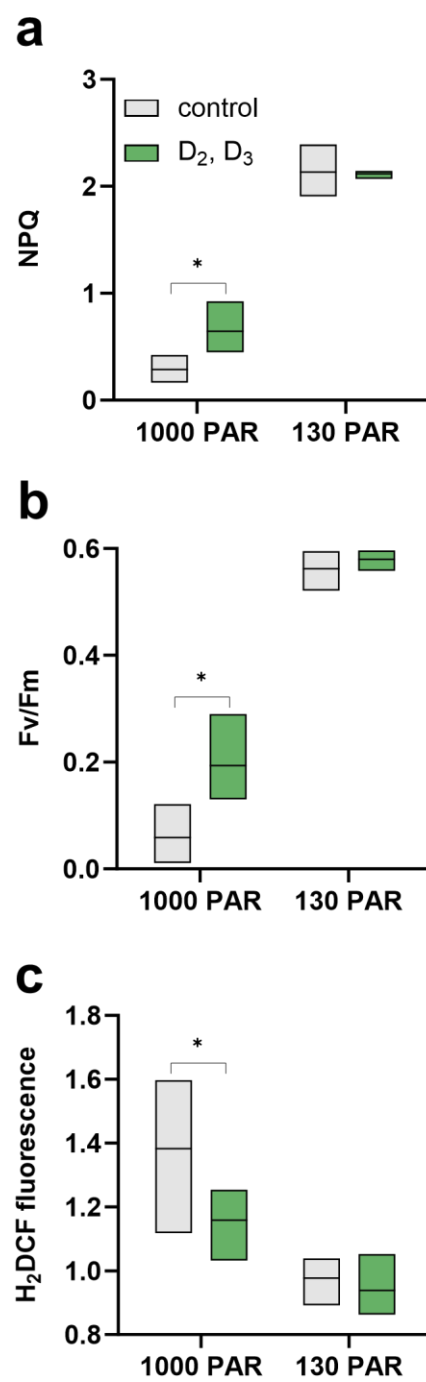


**Figure 2. Vitamin D treatment improves photosynthetic performance and alleviates oxidative stress following exposure to excess light.** (a) Non photochemical quenching (NPQ) and (b) F<sub>v</sub>/F<sub>m</sub> values of vitamin D-treated and control algae, exposed to regular (130 PAR) or excess (1000 PAR) light intensities. (c) Fluorescence values of vitamin D-treated and control algae stained with the intracellular reactive oxygen species (ROS) probe H<sub>2</sub>DCF-DA, exposed to regular (130 PAR) or excess light (1000 PAR) intensities. Statistically significant values ( $P < 0.05$ ) compared to control are marked by \*, calculated from three biological replicates using two-tailed paired t-test for (a,b) and one-tailed paired t-test for (c).

195 algal cells under excess light conditions, demonstrating that vitamin D is involved in mitigating  
196 ROS-induced oxidative stress.

197

198 **Discussion**

199 The current study reveals the photoprotective role of vitamin D in a globally abundant marine  
200 algal species. Our findings introduce a novel cellular mechanism that utilizes the photochemical  
201 transformation of vitamin D as an indicator of exposure to harmful radiation, consequently  
202 enhancing the algal physiological response to excess-light stress. This enhanced response is  
203 manifested by an increase in photosynthetic efficiency following exposure to conditions that  
204 inhibit photosynthesis, along with an overall reduction in the development of ROS (Fig. 2).  
205 Furthermore, the elevation in NPQ observed after vitamin D treatment, coupled with the  
206 upregulation of LHC3R, suggests that a significant aspect of the response triggered by vitamin  
207 D is aimed at mitigating photo-oxidative stress. Additionally, the fact that the physiological  
208 response in *E. huxleyi* algae to vitamin D is only observed following saturating light conditions  
209 may hint at a light-dependent regulatory mechanism.

210 Vitamin D can serve as a sensitive light indicator in phytoplankton. For example, phytoplankton  
211 residing in surface mixed layers of oceans often encounter significant fluctuations in PAR  
212 intensity throughout the day. These environments, which can extend depths of over 200  
213 meters<sup>66</sup>, may result in cells being transported over considerable vertical distances<sup>67</sup>, leading to  
214 rapid change in light intensity of hundreds of PAR within a matter of hours<sup>33,68</sup>. In such a dynamic  
215 scenario, as cells ascend, they experience an increase in UV-B and subsequently may generate  
216 vitamin D. The specificity of the photochemical conversion of vitamin D under UV-B wavelengths,  
217 coupled with its relatively high photochemical quantum yield<sup>69</sup>, suggests that it could function as  
218 an independent and sensitive proxy for assessing exposure to UV-B radiation, high light levels,  
219 or fluctuations in light intensity.

220 Interestingly, the impact of vitamin D on gene expression became evident only under a combined  
221 treatment with D<sub>2</sub> and D<sub>3</sub> (Fig. 1). Similarly, the combined treatment led to a lower cell density  
222 compared to separate D<sub>2</sub> or D<sub>3</sub> treatments (Fig S2). Decreased cell densities might be a result  
223 of cell cycle arrest, which is a phenomenon previously described in *E. huxleyi*<sup>70</sup> and is known to

224 occur in response to UV radiation across various organisms<sup>71-73</sup>. Whether vitamin D influences  
225 the algal cell cycle, and why a combination of D<sub>2</sub> and D<sub>3</sub> drives a detectable response, merits  
226 further investigation.

227 When studying algal physiology, it is essential to acknowledge the significance of UV-B as an  
228 influential environmental factor. In experimental setups aimed at studying algal physiology and  
229 ecology, UV-B radiation has traditionally been excluded due to its detrimental effects. However,  
230 this contradicts the natural conditions in which algae thrive, where they regularly encounter low  
231 levels of UV-B. While the omission of UV-B simplifies experimental conditions for precise  
232 variable isolation, our study unveils the profound influence of vitamin D, a product of UV-B  
233 exposure, on the physiological response of *E. huxleyi* to environmental stress. These findings  
234 shed light on the potentially advantageous role of UV-B for algae facing excess-light stress,  
235 encouraging further exploration of the interplay between algae and this often-overlooked  
236 environmental factor.

237 Our study offers comparative insights on the role of vitamin D in vertebrates and in *E. huxleyi*  
238 algae. The extensive knowledge on vitamin D biology primarily originates from research on  
239 humans and other vertebrates. Transposing this knowledge to *E. huxleyi* presents challenges  
240 due to significant phylogenetic and physiological differences between multicellular organisms  
241 and unicellular entities. Nevertheless, parallels can be drawn. Vitamin D was shown to enhance  
242 cellular defense in human and mice keratinocytes against UV-induced oxidative stress and DNA  
243 damage<sup>53,54</sup>. Vitamin D has also been shown to mitigate oxidative stress in rat liver and  
244 intestine<sup>50,74</sup>, partly through the upregulation of heme oxygenase, a response mirrored in vitamin  
245 D-treated algal cells. Furthermore, the upregulation by vitamin D of certain genes in *E. huxleyi*,  
246 potentially involved in intracellular signaling cascades (Fig. 2c, d), suggests the involvement of  
247 vitamin D in initiating or contributing to signaling mechanisms. In mammals, vitamin D plays a  
248 role in the activation of key signaling proteins, such as phospholipase C (PLC), phospholipase  
249 A<sub>2</sub> (PLA<sub>2</sub>) and phosphatidylinositol-3 kinase (PI3K)<sup>75</sup>, which are essential for the rapid generation  
250 of secondary messengers such as Ca<sup>2+</sup> and IP<sub>3</sub>. While *E. huxleyi* cells demonstrated the  
251 upregulation of PLC, PLA<sub>2</sub>, and PI3K following prolonged UV exposure (Table 1), further  
252 investigation is needed to determine if vitamin D also participates in regulating these proteins in  
253 algae. Interestingly, the involvement of Ca<sup>2+</sup> signaling in photo-oxidative stress mitigation has

254 been reported in other marine algal species<sup>76</sup>. Another possible similarity between vertebrates  
255 and *E. huxleyi* is the activation of vitamin D. In vertebrates, vitamin D requires enzymatic  
256 modifications to become hormonally active. These modifications include the hydroxylation of the  
257 1<sup>st</sup> and 25<sup>th</sup> carbons, to produce 1,25-(OH)<sub>2</sub>-vitamin D<sup>4</sup>. Similar hydroxylated D<sub>2</sub> and D<sub>3</sub> species  
258 were identified in the current research (Fig. S5) based on multiple reaction monitoring (MRM)  
259 profiles published previously<sup>77</sup>. Additional work is necessary to validate the detection of these  
260 hydroxylated species and the corresponding biosynthetic pathways in algae.

261 Vitamin D synthesis likely has ancient origins, given its presence across various lineages of  
262 eukaryotes<sup>9-15</sup>. Sterols are a defining feature of eukaryotes, and the enzymatic pathways leading  
263 to the production of ergosterol and 7-dehydrocholesterol, which are precursor molecules to D<sub>2</sub>  
264 and D<sub>3</sub> forms of vitamin D, may have existed in the last eukaryotic common ancestor (LECA)<sup>78,79</sup>.  
265 Consequently, it can be hypothesized that the earliest eukaryotes were already synthesizing  
266 vitamin D when exposed to solar radiation. While previous studies had postulated the ancient  
267 evolutionary origins of vitamin D<sup>20,80</sup>, the understanding of its role beyond the animal kingdom  
268 had remained limited. Eukaryotes rely on oxygen (O<sub>2</sub>), and their evolution is thought to have  
269 necessitated proximity to oxygenic photoautotrophs inhabiting the sunlit ocean surface<sup>81</sup>. This is  
270 because during their proposed emergence in the late Archean to early Proterozoic eras<sup>82,83</sup>, the  
271 deep ocean was likely devoid of O<sub>2</sub><sup>84-86</sup>. Considering the antioxidant properties exhibited by  
272 vitamin D in both animals and *E. huxleyi* algae, coupled with its evolutionary links to oxidative  
273 agents such as UV-B and O<sub>2</sub>, it prompts the question of whether vitamin D evolved in early  
274 eukaryotes as a means of sensing oxidative environments. A similar evolutionary role has been  
275 proposed to sterols, and chiefly to cholesterol that has been widely studied in the context of  
276 environmental O<sub>2</sub><sup>87,88</sup>. Like sterols, vitamin D possibly played a role in the early stages of life on  
277 Earth.

278

## 279 **Materials and methods**

### 280 Algal strain and growth conditions

281 The axenic algal strain of *E. huxleyi* CCMP3266 was purchased from the National Center for  
282 Marine Algae and Microbiota (Bigelow Laboratory for Ocean Sciences, Maine, USA). Algae were  
283 grown in artificial sea water according to Goyet and Poisson<sup>89</sup> and supplemented with L1

284 medium according to Guillard and Hargraves<sup>90</sup>, with the exception that  $\text{Na}_2\text{SiO}_3$  was omitted  
285 following the cultivation recommendations for this strain. Algae were grown in standing cultures  
286 in borosilicate Erlenmeyer flasks with an initial inoculum of 330 cells/ml, placed in a growth  
287 chamber at 18°C under a light/dark cycle of 16/8 hr. PAR intensity during the light period was  
288 130  $\mu\text{moles photons m}^{-2} \text{s}^{-1}$ . Cultures volume was 50 ml except for cultures used to measure  
289 growth under vitamin D treatment (Fig. S3) which were grown in 20 ml.

290 Continuous UV irradiation was achieved by placing a UV-emitting light source (Exo Terra Reptile  
291 UVB150, Hagen, Montreal, Canada) inside the algal growth chamber. Algal cultures experienced  
292 UV-A intensity of 0.5  $\text{w/m}^2$ , UV-B intensity of 0.07  $\text{w/m}^2$  and UV-C intensity of 0.026  $\text{w/m}^2$ ,  
293 measured using an ALMENO 2570 device (Ahlborn, Budapest, Hungary) placed within the  
294 Erlenmeyer flask. The UV-B intensity used in this study was selected to replicate the average  
295 UV-B radiation encountered at the ocean surface<sup>29</sup>. The UV light-source was operating daily for  
296 14 hours in parallel to the PAR light period, starting one hour after PAR illumination started, and  
297 ending one hour before PAR illumination ended. This irradiation regime aimed to mimic a  
298 simplified day cycle including dawn and dusk periods.

299 Algal growth was monitored by a CellStream CS-100496 flow cytometer (Merck, Darmstadt,  
300 Germany) using a 561 nm laser and plotting the chlorophyll fluorescence at 702/87 nm against  
301 side scatter.

### 302 Vitamin D treatment

303 Cultures were treated with 1  $\mu\text{M}$  of vitamin D<sub>2</sub> or D<sub>3</sub> (Sigma-Aldrich, Burlington, Massachusetts,  
304 USA) dissolved in DMSO, as this was the minimal vitamin D concentration in which an effect  
305 was observed on algal growth (Fig. S3b). For combined D<sub>2</sub> and D<sub>3</sub> treatment, 0.5  $\mu\text{M}$  of each  
306 species was added. The final DMSO concentration in cultures was 0.1%. Control cultures were  
307 treated with an equal amount of DMSO.

### 308 Vitamin D analysis

309 Metabolic analysis was conducted following Oberson<sup>77</sup>. Standards for D<sub>2</sub>, D<sub>3</sub>, ergosterol and 7-  
310 dehydrocholesterol were purchased in dry (Sigma-Aldrich) and dissolved in  $\text{CHCl}_3$ . Standard  
311 solutions of the different metabolites were combined into a single solution and diluted to create  
312 a standard curve. All final standards and samples were spiked with 50 ng of vitamin D2-d<sub>3</sub>

313 (IsoSciences, Ambler, Pennsylvania, USA) serving as an internal standard. Algal samples were  
314 centrifuged, lyophilized and stored in -80°C until analysis. Saponification was achieved by  
315 resuspending samples in 108 µl 55% KOH, 192 µl ethanol, and 60 µl of 9% NaCl and 7.4%  
316 ascorbic acid, followed by homogenization and stirring at room temperature for 18 hours.  
317 Samples were then supplemented with 40 µl 10% NaCl and 300 µl of 20% ethyl acetate in  
318 heptane, vortexed extensively and centrifuged for 30 minutes. The upper phase was collected,  
319 and the process was repeated twice. Samples were evaporated, dissolved in 200 µl of 0.5%  
320 isopropanol in hexane and sonicated. Strata Si-silica 55 µm 70 Å columns (Phenomenex,  
321 Torrance, California, USA) were used for solid phase extraction and were pre-conditioned with  
322 1 ml of 50% CHCl<sub>3</sub> in isopropanol, followed by two washes with 1 ml of hexane. Samples were  
323 then loaded onto the columns and washed with 0.5 ml of 0.5% isopropanol in hexane which were  
324 discarded, and washed again with 2.5 ml of 2.5% isopropanol in hexane which were  
325 collected. Samples were evaporated and dissolved in 200 µl of PTAD in acetonitrile, sonicated,  
326 stirred at room temperature for 2 hours, centrifuged for 10 minutes and transferred into LC-MS  
327 vials. Samples were protected from light as much as possible during the extraction process.

328 Due to the inconsistency in identification of D<sub>3</sub> in algal samples, several technical adaptations  
329 regarding algal growth and sample collection were implemented and evaluated. To examine  
330 whether inconsistencies arise due to rapid D<sub>3</sub> enzymatic degradation, algal cultures were  
331 immediately placed on ice, centrifuged in a cooled, 4°C centrifuge, and the supernatant quickly  
332 discarded and replaced with 50% methanol in DDW. The samples were then plunged into liquid  
333 nitrogen and stored in -80°C. Later, samples were thawed, evaporated in vacuum to remove the  
334 methanol, lyophilized and proceeded to vitamin D extraction. Additional modifications included  
335 increasing the intensity of UV-B radiation during algal growth, increasing sample size by  
336 combining separate cultures, and using F/2 trace metals instead of L1 trace metals. These  
337 attempts did not improve the reproducibility of D<sub>3</sub> detection.

338 Vitamin D was measured by UPC2-ESI-MS/MS equipped with Acquity UPC2 system (Waters,  
339 Milford, Massachusetts, USA). The MS detector (Waters TQ-XS) was equipped with an ESI  
340 source. The measurements were performed in the positive ionization mode using MRM. The  
341 source and de-solvation temperatures were maintained at 150°C and 500°C, respectively. The  
342 capillary voltage was set to 1.5 kV. Nitrogen was used as the de-solvation gas and cone gas at

343 a flow rate of 700 L h<sup>-1</sup> and 150 L h<sup>-1</sup>, respectively. Ionization parameters of ergosterol, 7-  
344 dehydrocholesterol, D<sub>2</sub> and D<sub>3</sub> were adjusted by direct infusion of standards. Ionization  
345 parameters for other compounds were taken from Oberson<sup>77</sup>.

346 UPC2 system: mobile phase A consisted of CO<sub>2</sub>, and mobile phase B consisted of 98% MeOH,  
347 2% DDW and 10mM ammonium formate. Make up solvent was 1% formic acid in 90% MeOH  
348 and 10% DDW at a flow rate of 0.4 ml min<sup>-1</sup>. The column (WATERS Acuity CSH FluoroPhenyl  
349 1.7 µm, 3.0x100 mm, cat. 186006573) was maintained at 45°C, injection volume was 3 µl. At the  
350 first 0.5 min of injection, 99.5% of mobile phase B, and 0.5% of mobile phase A were run at flow  
351 rate of 2.0 ml min<sup>-1</sup>. Then, mobile phase A was gradually reduced to 92% at 6 min, and further  
352 decreased to 70% at a flow rate of 1.75 ml min<sup>-1</sup> at 6.5 min. This composition of mobile phase  
353 and flow rate were kept until 7 min, followed by increase in mobile phase A to 99.5% at 7.8 min,  
354 and then increase in flow rate to 2 ml min<sup>-1</sup> at 8.5 min, and running at those conditions until 9  
355 min.

356 RNA extraction

357 Algal cultures were harvested for RNA extraction by centrifugation at 4000 rpm for 5 min at 18°C.  
358 RNA was extracted using the Isolate II RNA mini kit (Meridian Bioscience, London, UK)  
359 according to manufacturer instructions. Cells were ruptured in RLT buffer containing 1% β-  
360 mercapto-ethanol by bead beating for 5 min at 30 mHz. RNA was then treated with 3 µl Turbo  
361 DNase (ThermoFisher, Waltham, MA, USA) in a 50 µl reaction volume, followed by a cleaning  
362 step using RNA Clean & Concentrator<sup>TM</sup>-5 kit (Zymo Research, Irvine, CA, USA) according to  
363 manufacturer instructions. RNA was used for generating transcriptomic data and qRT-PCR  
364 analysis.

365 Transcriptomic analysis

366 Transcriptomic data was generated using the MARS-seq library preparation protocol<sup>91</sup>, and  
367 analyzed with the UTAP pipeline<sup>92</sup>. As part of the pipeline, read counts for each gene were  
368 normalized using the DESeq2's median of ratios method<sup>93</sup>. Differential expression (DE) between  
369 treatments was calculated using the following thresholds: mean number of normalized reads  
370 across all samples ≥ 5, adjusted p-value ≤ 0.05, Log2 fold change ≤ -0.7 or ≥ 0.7. The previously  
371 generated *E. huxleyi* CCMP3226 synthetic genome (sGenome) and annotation file was used as

372 reference for the UTAP pipeline<sup>94</sup>. Briefly, the *E. huxleyi* CCMP3226 sGenome was generated  
373 by *de novo* transcriptome assembly of short-reads and long-reads. The assembled *E. huxleyi*  
374 CCMP3226 transcripts were then mapped to the *E. huxleyi* CCMP1516 reference genome<sup>95</sup> to  
375 define gene loci. For the current work, functional gene annotations were manually curated by  
376 identifying open reading frames in assembled transcripts using the ORF finder tool  
377 ([www.ncbi.nlm.nih.gov/orffinder](http://www.ncbi.nlm.nih.gov/orffinder); transcript accessions are given in Table S1) and analyzing  
378 protein domains in the translated sequences using InterProScan 5<sup>96</sup>. Additionally, transcript  
379 sequences were searched against the swissprot database using NCBI blastx<sup>97</sup>, and the hit with  
380 the highest E-value taken. Specifically, the gene loci analyzed using blastx were G18590,  
381 sharing highest similarity to *Chlamydomonas reinhardtii* LHCSR (NCBI accession P93664.1)  
382 with E-value of 1e-26 and nucleotide identity of 57%; G25467, sharing highest similarity to rat  
383 *cyp1a2* (NCBI accession P04799.2) with E-value of 1e-31 and nucleotide identity of 27%;  
384 G14502, sharing highest similarity to *Arabidopsis thaliana* Calmodulin-like protein 12 (NCBI  
385 accession P25071.3) with E-value of 6e-5 and nucleotide identity of 22.6%. The putative Ca-  
386 binding activity of G26534 was assessed by identifying *bona fide* Ca-binding domains using  
387 InterProScan 5. Specifically, we performed blastx<sup>97</sup> and focused on the highest hit that contained  
388 an identifiable protein domain using InterProScan 5<sup>96</sup>, resulting in the identification of an EF-  
389 hand family protein in *Chrysochromulina tobini* that harbors three EF-hand domain pairs (NCBI  
390 accession KOO34173.1, with E-value of 8e-13 and nucleotide identity of 32%).

391 Quantitative real time PCR (qRT-PCR)

392 Algal cultures were treated with vitamin D as described earlier. UV-treated cultures were  
393 exposed to the same UV intensities as described above and treated with equal amounts of  
394 DMSO. All treatments lasted 1 hour. Equal concentrations of RNA taken from 10 days old  
395 cultures were utilized for cDNA synthesis using Superscript IV (ThermoFisher), according to  
396 manufacturer instructions. qPCR was conducted in 384 well plates using SensiFAST SYBR Lo-  
397 ROX Kit (Meridian Bioscience, Cincinnati, OH, USA) in a QuantStudio 5 qPCR cycler (Applied  
398 Biosystems, Foster City, CA, USA). The qPCR program ran according to enzyme requirements  
399 for 40 cycles. Samples were normalized using three housekeeping genes: *alpha-tubulin*, *beta-  
400 tubulin* and *ribosomal protein l13 (rpl13)*. DNA contamination was assessed by applying the  
401 same program on RNA samples that were not reverse transcribed (omitting the Superscript IV

402 enzyme in the reverse transcription reaction mix). Gene expression ratios were analyzed  
403 according to Vandesompele<sup>98</sup> by geometric averaging of housekeeping genes. Relative gene  
404 expression levels were compared to control samples. Primer efficiencies were determined using  
405 the QuantStudio 5 software, by qPCR amplification of serially diluted cDNA. All primers had a  
406 measured efficiency between 80-120%. Primer sequences are given in Table S2.

407 Chlorophyll fluorescence

408 Algal cultures were divided into four subcultures that were subjected to one of four treatments:  
409 1000 PAR with or without vitamin D (as described earlier) and 130 PAR with or without vitamin  
410 D. Chlorophyll A fluorescence parameters were estimated following 2 hours of treatment.  
411 Parameters were estimated by pulse amplitude-modulated fluorometry using WATER-PAM II  
412 (Heinz Walz GmbH, Effeltrich, Germany). Maximum photosystem II quantum yield ( $F_v/F_m$ ) was  
413 calculated as  $F_v/F_m = (F_m - F_0) / F_m^{64}$ , where  $F_0$  is the baseline fluorescence under a measuring  
414 light of 160 PAR and  $F_m$  is the maximum fluorescence measured with a 0.9 s saturating light  
415 pulse of 6000  $\mu\text{mol photons m}^{-2} \text{s}^{-1}$ . Non-photochemical quenching (NPQ) was calculated as  
416  $\text{NPQ} = (F_m - F'_m) / F'_m^{63}$ , where  $F_m$  was the maximum fluorescence yield after dark adaptation  
417 and  $F'_m$  the maximum fluorescence yield under actinic light of 1150 PAR. Prior to analysis, algal  
418 samples were dark-adapted for 5 minutes. No major difference in  $F_v/F_m$  was observed between  
419 algae that were dark-adapted for 5 or 30 minutes following exposure to regular light (Fig. S6),  
420 suggesting that a darkness period of 5 minutes sufficiently relaxed PSII reaction centers.

421 Intracellular reactive oxygen species (ROS) measurements

422 Algal cultures were divided into subcultures and treated as described under 'chlorophyll  
423 fluorescence'. Vitamin D-treated and control cultures were placed in a growth chamber and  
424 exposed to either regular light conditions (130 PAR) or to high-light conditions (1000 PAR) for 5  
425 hours. For intracellular ROS assessment, cultures were stained with 0.5  $\mu\text{M}$  of H<sub>2</sub>DCFDA  
426 (ThermoFisher) in DMSO. Staining was performed 2 hours after the start of the treatment, and  
427 cultures were left in the dark for 20 minutes before they were introduced back into the growth  
428 chamber for the remaining 3 hours. Samples were measured using CellStream CS-100496,  
429 excited at 488 nm and the signal was collected at 528/46 nm. The algal population was gated  
430 by plotting chlorophyll fluorescence (excitation-emission 561-702/87 nm) against side scatter.

431

432 **Acknowledgments**

433 We appreciate the technical guidance of Dr. Shifra Ben-Dor, Dr. Merav Kedmi and Dr. Hadas  
434 Keren-Shaul in RNA-sequencing and are thankful for the help of Dr. Ron Rotkopf with statistical  
435 analysis, and of Dr. Alexander Brandis with LC-MS analysis (Life Sciences Core Facilities,  
436 Weizmann Institute of Science, Israel). We thank Dr. Shilo Rosenwasser (The Hebrew University  
437 of Jerusalem, Israel) for sharing his expertise in pulse amplitude-modulated fluorometry. We  
438 thank Prof. Robert Fluhr and Prof. Dan Yakir (Weizmann Institute of Science, Israel) for valuable  
439 comments during the study. We are grateful for Dr. Sheera Adar and Yuval Cohen (The Hebrew  
440 University of Jerusalem, Israel) for their insights into UV-induced DNA damage, and to Dr. Chana  
441 Kranzler (Bar Ilan University, Israel) for her technical and scientific support. Finally, we thank all  
442 members of the Segev lab for insightful discussions and input. O.E. received the Sustainability  
443 and Energy Research Initiative (SAERI) fellowship. The study was supported by funds received  
444 from the Minerva Foundation with funding from the German Federal Ministry for Education and  
445 Research, the Israel Science Foundation (ISF 947/18), the European Research Council (ERC  
446 StG 101075514) and the de Botton center for marine sciences, granted to E.S.

447

448 **Authors Contributions**

449 O.E. and E.S. designed the study. O.E., S.M. and I.P. performed and analyzed experiments.  
450 O.E., E. F. and M.S. performed computational analyses. O.E. and E.S. wrote the manuscript. All  
451 authors discussed the results and contributed to the final manuscript.

452

453 **Competing interests**

454 The authors declare no competing interests.

455

456

457 **References**

- 458 1. Havinga, E. Vitamin D, example and challenge. *Experientia* **29**, 1181–1193 (1973).
- 459 2. Holick, M. F. *et al.* Photosynthesis of Previtamin D3 in Human Skin and the Physiologic  
460 Consequences. *Science* **210**, 203–205 (1980).
- 461 3. Kalaras, M. D., Beelman, R. B., Holick, M. F. & Elias, R. J. Generation of potentially bioactive  
462 ergosterol-derived products following pulsed ultraviolet light exposure of mushrooms (*Agaricus*  
463 *bisporus*). *Food Chem.* **135**, 396–401 (2012).
- 464 4. Hossein-Nezhad, A. & Holick, M. F. Vitamin D for health: A global perspective. *Mayo Clin. Proc.*  
465 **88**, 720–755 (2013).
- 466 5. Fukumoto, S. Phosphate metabolism and vitamin D. *Bonekey Rep.* **3**, 497 (2014).
- 467 6. Veldurthy, V. *et al.* Vitamin D, calcium homeostasis and aging. *Bone Res.* **4**, 1–7 (2016).
- 468 7. Lopez Payares, G. M. & Ali, F. A. Vitamin D deficiency. *5-Minute Clin. Consult Stand. 2016*  
469 *Twenty Fourth Ed.* 266–281 (2015).
- 470 8. Schwalfenberg, G. K. A review of the critical role of vitamin D in the functioning of the immune  
471 system and the clinical implications of vitamin D deficiency. *Mol. Nutr. Food Res.* **55**, 96–108  
472 (2011).
- 473 9. Ljubic, A., Thulesen, E. T., Jacobsen, C. & Jakobsen, J. UVB exposure stimulates production of  
474 vitamin D3 in selected microalgae. *Algal Res.* **59**, 102472 (2021).
- 475 10. Brown, M. R., Mular, M., Miller, I., Farmer, C. & Trenerry, C. The vitamin content of microalgae  
476 used in aquaculture. *J. Appl. Phycol.* **11**, 247–255 (1999).
- 477 11. Holick, M. F., Holick, S. A. & Guillard, R. L. Photosynthesis of previtamin D in phytoplankton.  
478 *Curr. trends Comp. Endocrinol.* **2**, 1263–1266 (1982).
- 479 12. Jäpel, R. B. & Jakobsen, J. Vitamin D in plants: a review of occurrence, analysis, and  
480 biosynthesis. *Front. Plant Sci.* **4**, 1–20 (2013).
- 481 13. Mattila, P. H., Piironen, V. I., Uusi-Rauva, E. J. & Koivistoinen, P. E. Vitamin D Contents in  
482 Edible Mushrooms. *J. Agric. Food Chem.* **42**, 2449–2453 (1994).
- 483 14. Hohman, E. E. *et al.* Bioavailability and Efficacy of Vitamin D2 from UV-Irradiated Yeast in  
484 Growing, Vitamin D-Deficient Rats. *J. Agric. Food Chem.* **59**, 2341–2346 (2011).
- 485 15. Wang, T., Bengtsson, G., Kärnefelt, I. & Björn, L. O. Provitamins and vitamins D2 and D3 in  
486 *Cladina* spp. over a latitudinal gradient: possible correlation with UV levels. *J. Photochem.*  
487 *Photobiol. B Biol.* **62**, 118–122 (2001).
- 488 16. Brocks, J. J. *et al.* The rise of algae in Cryogenian oceans and the emergence of animals. *Nature*  
489 **548**, 578–581 (2017).
- 490 17. Rao, D. S. & Raghuramulu, N. Food chain as origin of vitamin D in fish. *Comp. Biochem. Physiol.*  
491 *- A Physiol.* **114**, 15–19 (1996).
- 492 18. Fraser, D. R. *Evolutionary Biology: Mysteries of Vitamin D in Fish. Vitamin D: Fourth Edition* **1**,  
493 (Elsevier Inc., 2018).
- 494 19. Atsuko, T., Toshio, O., Makoto, T. & Tadashi, K. Possible origin of extremely high contents of

vitamin D3 in some kinds of fish liver. *Comp. Biochem. Physiol. Part A Physiol.* **100**, 483–487 (1991).

20. Bikle, D. D. Vitamin D: An ancient hormone. *Exp. Dermatol.* **20**, 7–13 (2011).
21. Rastogi, R. P., Richa, Kumar, A., Tyagi, M. B. & Sinha, R. P. Molecular Mechanisms of Ultraviolet Radiation-Induced DNA Damage and Repair. *J. Nucleic Acids* **2010**, 592980 (2010).
22. de Jager, T. L., Cockrell, A. E. & Du Plessis, S. S. Ultraviolet Light Induced Generation of Reactive Oxygen Species. in *Ultraviolet Light in Human Health, Diseases and Environment* 15–23 (2017). doi:10.1007/978-3-319-56017-5\_2
23. Czégény, G., Mátkai, A. & Hideg, É. UV-B effects on leaves—Oxidative stress and acclimation in controlled environments. *Plant Sci.* **248**, 57–63 (2016).
24. Tron, V. A. *et al.* p53-regulated apoptosis is differentiation dependent in ultraviolet B- irradiated mouse keratinocytes. *Am. J. Pathol.* **153**, 579–585 (1998).
25. Kataria, S., Jajoo, A. & Guruprasad, K. N. Impact of increasing Ultraviolet-B (UV-B) radiation on photosynthetic processes. *J. Photochem. Photobiol. B Biol.* **137**, 55–66 (2014).
26. Szilárd, A., Sass, L., Deák, Z. & Vass, I. The sensitivity of Photosystem II to damage by UV-B radiation depends on the oxidation state of the water-splitting complex. *Biochim. Biophys. Acta - Bioenerg.* **1767**, 876–882 (2007).
27. Morris, D. P. *et al.* The attenuation of solar UV radiation in lakes and the role of dissolved organic carbon. *Limnol. Oceanogr.* **40**, 1381–1391 (1995).
28. Tedetti, M. & Sempéré, R. Penetration of Ultraviolet Radiation in the Marine Environment. A Review. *Photochem. Photobiol.* **82**, 389 (2006).
29. Häder, D. P. Penetration and effects of solar UV-B on phytoplankton and macroalgae. in *UV-B and Biosphere* 4–13 (1997). doi:10.1007/978-94-011-5718-6\_1
30. Bendif, E. M. *et al.* Repeated species radiations in the recent evolution of the key marine phytoplankton lineage *Gephyrocapsa*. *Nat. Commun.* **10**, 4234 (2019).
31. Taylor, A. R., Brownlee, C. & Wheeler, G. Coccolithophore Cell Biology: Chalking Up Progress. *Ann. Rev. Mar. Sci.* **9**, 283–310 (2017).
32. Paasche, E. A review of the coccolithophorid *emiliania huxleyi* (prymnesiophyceae), with particular reference to growth, coccolith formation, and calcification-photosynthesis interactions. *Phycologia* **40**, 503–529 (2001).
33. Nanninga, H. J. & Tyrrell, T. Importance of light for the formation of algal blooms by *Emiliania huxleyi*. *Mar. Ecol. Prog. Ser.* **136**, 195–203 (1996).
34. Volkman, J. K., Smith, D. J., Eglinton, G., Forsberg, T. E. V. & Corner, E. D. S. Sterol and fatty acid composition of four marine haptophycean algae. *J. Mar. Biol. Assoc. United Kingdom* **61**, 509–527 (1981).
35. Eltgroth, M. L., Watwood, R. L. & Wolfe, G. V. Production and cellular localization of neutral long-chain lipids in the haptophyte algae *isochrysis galbana* and *emiliania huxleyi*. *J. Phycol.* **41**, 1000–1009 (2005).
36. Sañé, E. *et al.* The Recent Advanced in Microalgal Phytosterols: Bioactive Ingredients Along With Human-Health Driven Potential Applications. *Food Rev. Int.* **39**, 1859–1878 (2023).

535 37. Jäpel, R. B., Silvestro, D., Smedsgaard, J., Jensen, P. E. & Jakobsen, J. Quantification of  
536 vitamin D3 and its hydroxylated metabolites in waxy leaf nightshade (*Solanum glaucophyllum*  
537 Desf.), tomato (*Solanum lycopersicum* L.) and bell pepper (*Capsicum annuum* L.). *Food Chem.*  
538 **138**, 1206–1211 (2013).

539 38. Berridge, M. J. The inositol trisphosphate/calcium signaling pathway in health and disease.  
540 *Physiol. Rev.* **96**, 1261–1296 (2016).

541 39. Di Costanzo, F., Di Dato, V., Ianora, A. & Romano, G. Prostaglandins in marine organisms: A  
542 review. *Mar. Drugs* **17**, (2019).

543 40. Seltmann, M. A. *et al.* Differential Impact of Lipoxygenase 2 and Jasmonates on Natural and  
544 Stress-Induced Senescence in *Arabidopsis*. *Plant Physiol.* **152**, 1940–1950 (2010).

545 41. Kaye, Y. *et al.* Inositol Polyphosphate 5-Phosphatase7 Regulates the Production of Reactive  
546 Oxygen Species and Salt Tolerance in *Arabidopsis*. *Plant Physiol.* **157**, 229–241 (2011).

547 42. Salmon, J. A. & Higgs, G. A. Prostaglandins and leukotrienes as inflammatory mediators. *Br.*  
548 *Med. Bull.* **43**, 285–296 (1987).

549 43. Wan S., Y., Wang Q., Z., Shao, Y., Voorhees J., J. & Fisher J., G. Ultraviolet irradiation activates  
550 PI 3-kinase/AKT survival pathway via EGF receptors in human skin in vivo. *Int J Oncol* **18**, 461–  
551 466 (2001).

552 44. Black, A. K., Greaves, M. W., Hensby, C. N. & Plummer, N. A. Increased prostaglandins E2 and  
553 F2alpha in human skin at 6 and 24 h after ultraviolet B irradiation (290- 320 nm). *Br. J. Clin.*  
554 *Pharmacol.* **5**, 431–436 (1978).

555 45. Moreno, J. *et al.* Regulation of prostaglandin metabolism by calcitriol attenuates growth  
556 stimulation in prostate cancer cells. *Cancer Res.* **65**, 7917–7925 (2005).

557 46. Trechsel, U., Carol M. Taylor, Jean-Philippe Bonjour & Fleisch, H. Influence of prostaglandins  
558 and of cyclic nucleotides on the metabolism of 25-hydroxyvitamin D3 in primary chick kidney cell  
559 culture. *Biochem. Biophys. Res. Commun.* **93**, 15–38 (1980).

560 47. Tang, W., Ziboh, V. A., Isseroff, R. R. & Martinez, D. Novel regulatory actions of 1 $\alpha$ ,25-  
561 dihydroxyvitamin D3 on the metabolism of polyphosphoinositides in murine epidermal  
562 keratinocytes. *J. Cell. Physiol.* **132**, 131–136 (1987).

563 48. De Boland, A. R., Facchinetto, M. M., Balogh, G., Massheimer, V. & Boland, R. L. Age-associated  
564 decrease in inositol 1,4,5-trisphosphate and diacylglycerol generation by 1,25(OH)2-vitamin D3  
565 in rat intestine. *Cell. Signal.* **8**, 153–157 (1996).

566 49. Bourdeau, A., Atmani, F., Grosse, B. & Lieberherr, M. Rapid effects of 1, 25-dihydroxyvitamin d3  
567 and extracellular ca2+ on phospholipid metabolism in dispersed porcine parathyroid cells.  
568 *Endocrinology* **127**, 2738–2743 (1990).

569 50. Wang, P.-F., Yao, D.-H., Hu, Y.-Y. & Li, Y. Vitamin D Improves Intestinal Barrier Function in  
570 Cirrhosis Rats by Upregulating Heme Oxygenase-1 Expression. *Biomol. Ther. (Seoul)*. **27**, 222–  
571 230 (2019).

572 51. Wu, X. *et al.* Vitamin D–vitamin D receptor alleviates oxidative stress in ischemic acute kidney  
573 injury via upregulating glutathione peroxidase 3. *FASEB J.* **37**, e22738 (2023).

574 52. Pavlovitch, J. H., Rizk, M. & Balsan, S. Vitamin D nutrition increases skin tyrosinase response to  
575 exposure to ultraviolet radiation. *Mol. Cell. Endocrinol.* **25**, 295–302 (1982).

576 53. Gordon-Thomson, C. *et al.* 1 $\alpha$ ,25 Dihydroxyvitamin D3 enhances cellular defences against UV-  
577 induced oxidative and other forms of DNA damage in skin. *Photochemical and Photobiological*  
578 *Sciences* **11**, 1837–1847 (2012).

579 54. Wong, C. T. & Oh, D. H. Vitamin D Receptor Promotes Global Nucleotide Excision Repair by  
580 Facilitating XPC Dissociation from Damaged DNA. *J. Invest. Dermatol.* **141**, 1656–1663 (2021).

581 55. Pinnola, A. *et al.* Light-Harvesting Complex Stress-Related Proteins Catalyze Excess Energy  
582 Dissipation in Both Photosystems of *Physcomitrella patens*. *Plant Cell* **27**, 3213–3227 (2015).

583 56. Peers, G. *et al.* An ancient light-harvesting protein is critical for the regulation of algal  
584 photosynthesis. *Nature* **462**, 518–521 (2009).

585 57. Tilbrook, K. *et al.* UV-B perception and acclimation in *chlamydomonas reinhardtii*. *Plant Cell* **28**,  
586 966–983 (2016).

587 58. Yannarelli, G. G., Noriega, G. O., Batlle, A. & Tomaro, M. L. Heme oxygenase up-regulation in  
588 ultraviolet-B irradiated soybean plants involves reactive oxygen species. *Planta* **224**, 1154–1162  
589 (2006).

590 59. Cui, W. *et al.* Haem oxygenase-1 is involved in salicylic acid-induced alleviation of oxidative  
591 stress due to cadmium stress in *Medicago sativa*. *J. Exp. Bot.* **63**, 5521–5534 (2012).

592 60. Applegate, L. A., Luscher, P. & Tyrrell, R. M. Induction of Heme Oxygenase: A General  
593 Response to Oxidant Stress in Cultured Mammalian Cells1. *Cancer Res.* **51**, 974–978 (1991).

594 61. Harris, G. N., Scanlan, D. J. & Geider, R. J. Acclimation of *Emiliania huxleyi* (Prymnesiophyceae)  
595 to photon flux density. *J. Phycol.* **41**, 851–862 (2005).

596 62. Xu, J. *et al.* The role of coccoliths in protecting *Emiliania huxleyi* against stressful light and UV  
597 radiation. 4637–4643 (2016). doi:10.5194/bg-13-4637-2016

598 63. Ruban, A. V. Nonphotochemical chlorophyll fluorescence quenching: Mechanism and  
599 effectiveness in protecting plants from photodamage. *Plant Physiol.* **170**, 1903–1916 (2016).

600 64. Genty, B., Briantais, J.-M. & Baker, N. R. The relationship between the quantum yield of  
601 photosynthetic electron transport and quenching of chlorophyll fluorescence. *Biochim. Biophys.*  
602 *Acta - Gen. Subj.* **990**, 87–92 (1989).

603 65. Vass, I., Cser, K. & Cheregi, O. Molecular Mechanisms of Light Stress of Photosynthesis. *Ann.*  
604 *N. Y. Acad. Sci.* **1113**, 114–122 (2007).

605 66. Carlson, D. F., Fredj, E. & Gildor, H. The annual cycle of vertical mixing and restratification in the  
606 Northern Gulf of Eilat/Aqaba (Red Sea) based on high temporal and vertical resolution  
607 observations. *Deep Sea Res. Part I Oceanogr. Res. Pap.* **84**, 1–17 (2014).

608 67. Chiswell, S., Calil, P. & Boyd, P. Spring blooms and annual cycles of phytoplankton: A unified  
609 perspective. *J. Plankton Res.* **37**, (2015).

610 68. Weller, R. A. & Price, J. F. Langmuir circulation within the oceanic mixed layer. *Deep Sea Res.*  
611 *Part A. Oceanogr. Res. Pap.* **35**, 711–747 (1988).

612 69. MacLaughlin, J. A., Anderson, R. R. & Holick, M. F. Spectral Character of Sunlight Modulates  
613 Photosynthesis of Previtamin D3 and Its Photoisomers in Human Skin. *Science* **216**, 1001–1003  
614 (1982).

615 70. Pollara, S. B. *et al.* Bacterial Quorum-Sensing Signal Arrests Phytoplankton Cell Division and

616 Impacts Virus-Induced Mortality. *mSphere* **6**, (2021).

617 71. Pavey, S., Russell, T. & Gabrielli, B. G2 phase cell cycle arrest in human skin following UV  
618 irradiation. *Oncogene* **20**, 6103–6110 (2001).

619 72. Jiang, L., Wang, Y., Björn, L. O. & Li, S. Does cell cycle arrest occur in plant under solar UV-B  
620 radiation? *Plant Signal. & Behav.* **6**, 892–894 (2011).

621 73. Rudolph, C. J., Upton, A. L. & Lloyd, R. G. Replication fork stalling and cell cycle arrest in UV-  
622 irradiated *Escherichia coli*. *Genes and Development* **21**, 668–681 (2007).

623 74. Özerkan, D., Özsoy, N., Akbulut, K. G., Güney, Ş. & Öztürk, G. The protective effect of vitamin D  
624 against carbon tetrachloride damage to the rat liver. *Biotech. Histochem.* **92**, 513–523 (2017).

625 75. Hii, C. S. & Ferrante, A. The Non-Genomic Actions of Vitamin D. *Nutrients* **8**, 135 (2016).

626 76. Flori, S. *et al.* Diatoms exhibit dynamic chloroplast calcium signals in response to high light and  
627 oxidative stress. *bioRxiv* 2008–2023 (2023).

628 77. Oberson, J. M., Bénet, S., Redeuil, K. & Campos-Giménez, E. Quantitative analysis of vitamin D  
629 and its main metabolites in human milk by supercritical fluid chromatography coupled to tandem  
630 mass spectrometry. *Anal. Bioanal. Chem.* **412**, 365–375 (2020).

631 78. Brocks, J. J. *et al.* Lost world of complex life and the late rise of the eukaryotic crown. *Nature*  
632 **618**, 767–773 (2023).

633 79. Desmond, E. & Gribaldo, S. Phylogenomics of Sterol Synthesis: Insights into the Origin,  
634 Evolution, and Diversity of a Key Eukaryotic Feature. *Genome Biol. Evol.* **1**, 364–381 (2009).

635 80. Carlberg, C. Vitamin D in the Context of Evolution. *Nutrients* **14**, (2022).

636 81. Waldbauer, J. R., Newman, D. K. & Summons, R. E. Microaerobic steroid biosynthesis and the  
637 molecular fossil record of Archean life. *Proceedings of the National Academy of Sciences of the*  
638 *United States of America* **108**, 13409–13414 (2011).

639 82. Knoll, A. H., Javaux, E. J., Hewitt, D. & Cohen, P. Eukaryotic organisms in Proterozoic oceans.  
640 *Philos. Trans. R. Soc. B Biol. Sci.* **361**, 1023–1038 (2006).

641 83. Han, T. M. & Runnegar, B. Megascopic Eukaryotic Algae from the 2.1-Billion-Year-Old  
642 Negaunee Iron-Formation, Michigan. *Science* **257**, 232–235 (1992).

643 84. Canfield, D. E. A new model for Proterozoic ocean chemistry. *Nature* **396**, 450–453 (1998).

644 85. Lyons, T. W., Reinhard, C. T. & Planavsky, N. J. The rise of oxygen in Earth's early ocean and  
645 atmosphere. *Nature* **506**, 307–315 (2014).

646 86. Anbar, A. D. & Knoll, A. H. Proterozoic ocean chemistry and evolution: A bioinorganic bridge?  
647 *Science* **297**, 1137–1142 (2002).

648 87. Smith, L. L. Another cholesterol hypothesis: cholesterol as antioxidant. *Free Radic. Biol. Med.*  
649 **11**, 47–61 (1991).

650 88. Galea, A. M. & Brown, A. J. Special relationship between sterols and oxygen: were sterols an  
651 adaptation to aerobic life? *Free Radic. Biol. Med.* **47**, 880–889 (2009).

652 89. Goyet, C. & Poisson, A. New determination of carbonic acid dissociation constants in seawater  
653 as a function of temperature and salinity. *Deep Sea Res. Part A. Oceanogr. Res. Pap.* **36**, 1635–  
654 1654 (1989).

655 90. Guillard, R. R. L. & Hargraves, P. E. *Stichochrysis immobilis* is a diatom, not a chrysophyte.  
656 *Phycologia* **32**, 234–236 (1993).

657 91. Keren-Shaul, H. *et al.* MARS-seq2.0: an experimental and analytical pipeline for indexed sorting  
658 combined with single-cell RNA sequencing. *Nat. Protoc.* **14**, 1841–1862 (2019).

659 92. Kohen, R. *et al.* UTAP: User-friendly Transcriptome Analysis Pipeline. *BMC Bioinformatics* **20**,  
660 154 (2019).

661 93. Love, M. I., Huber, W. & Anders, S. Moderated estimation of fold change and dispersion for  
662 RNA-seq data with DESeq2. *Genome Biol.* **15**, 550 (2014).

663 94. Sperfeld, M., Segev, E. & Dayana Yahalomi. Resolving the microalgal gene landscape at the  
664 strain level: A novel hybrid transcriptome of *Emiliania huxleyi* CCMP3266. *Appl. Environ.*  
665 *Microbiol.* (2021). doi:10.1128/AEM.01418-21

666 95. Read, B. A. *et al.* Pan genome of the phytoplankton *Emiliania* underpins its global distribution.  
667 *Nature* **499**, 209–213 (2013).

668 96. Jones, P. *et al.* InterProScan 5: genome-scale protein function classification. *Bioinformatics* **30**,  
669 1236–1240 (2014).

670 97. Sayers, E. W. *et al.* Database resources of the national center for biotechnology information.  
671 *Nucleic Acids Res.* **50**, D20–D26 (2022).

672 98. Vandesompele, J. *et al.* Accurate normalization of real-time quantitative RT-PCR data by  
673 geometric averaging of multiple internal control genes. *Genome Biol.* **3**, research0034.1 (2002).

674

675

676

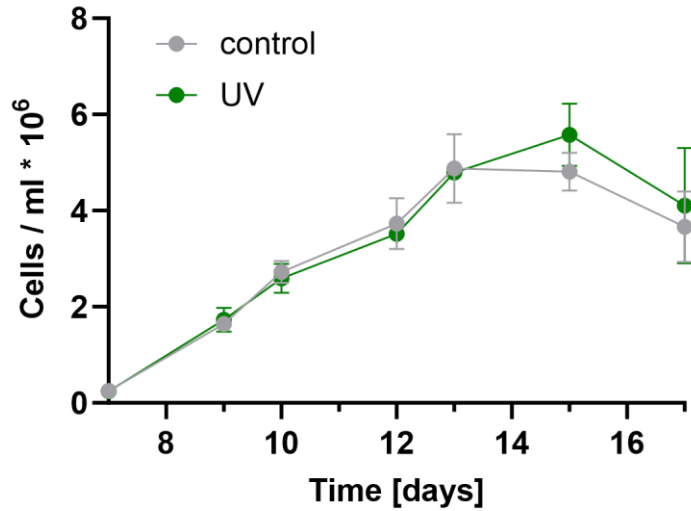


**Figure S1. Continuous UV irradiation during the light period did not affect algal growth.**  
Growth curves of the algal cultures that were grown under control and UV regime and were used for generating the transcriptomic data. Cell density was measured from day 7. Error bars indicate standard deviation based on 3 biological replicates.

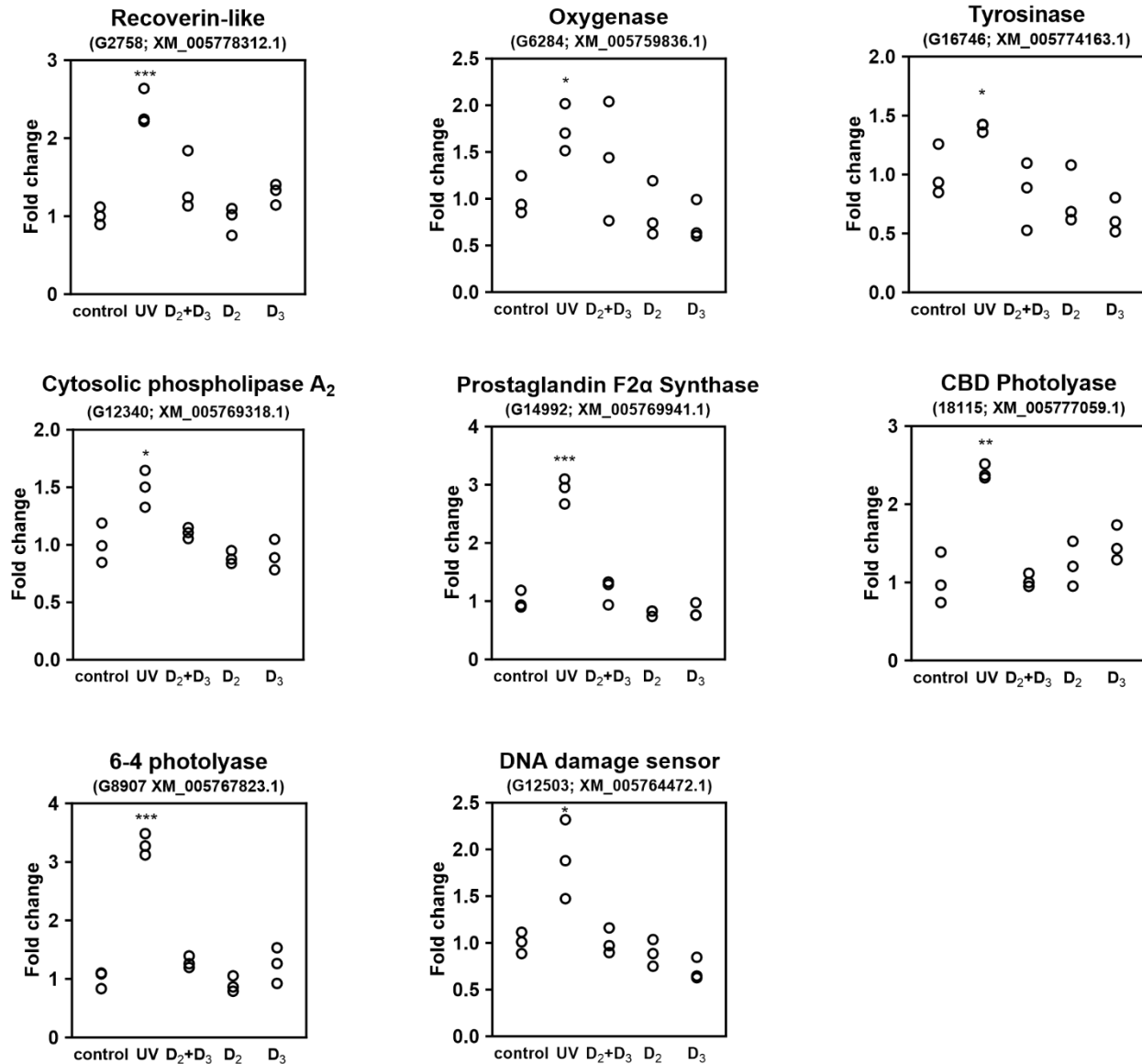


**Figure S2. UV radiation causes upregulation of various signaling and stress-response mechanisms.** qRT-PCR analysis of genes under 1 hour of UV exposure or vitamin D treatments. Top title denotes gene products. In brackets: gene identifier in *E. huxleyi*; matching gene in *E. huxleyi* CCMP1516 reference genome<sup>95</sup>. Statistical significance compared to control was calculated using two-tailed t-test assuming equal variances. One, two or three asterisks indicate  $P < 0.05$ ,  $P < 0.01$  and  $P < 0.001$ , respectively.

678

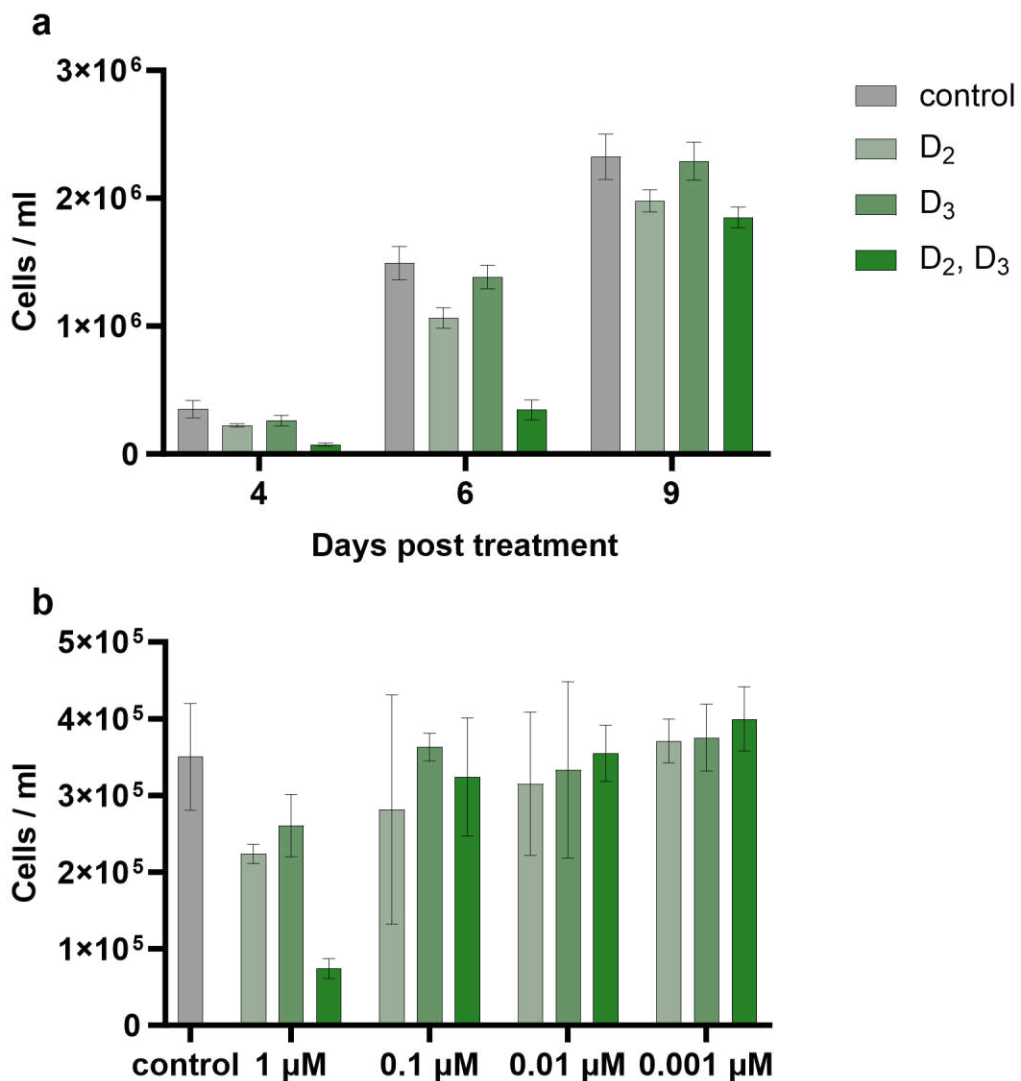


**Figure S3. The combined treatment of vitamin D<sub>2</sub> and D<sub>3</sub> has a synergistic effect on algal growth, outperforming individual D<sub>2</sub> or D<sub>3</sub> application.** (a) Growth dynamics of algal cultures treated with 1 μM of vitamin D species. (b) Variation in algal cell densities after 4 days of treatment with different concentrations of vitamin D<sub>2</sub>, D<sub>3</sub>, and both (indicated by the green shades in the figure legend). Error bars indicate standard deviation from 3 biological replicates.

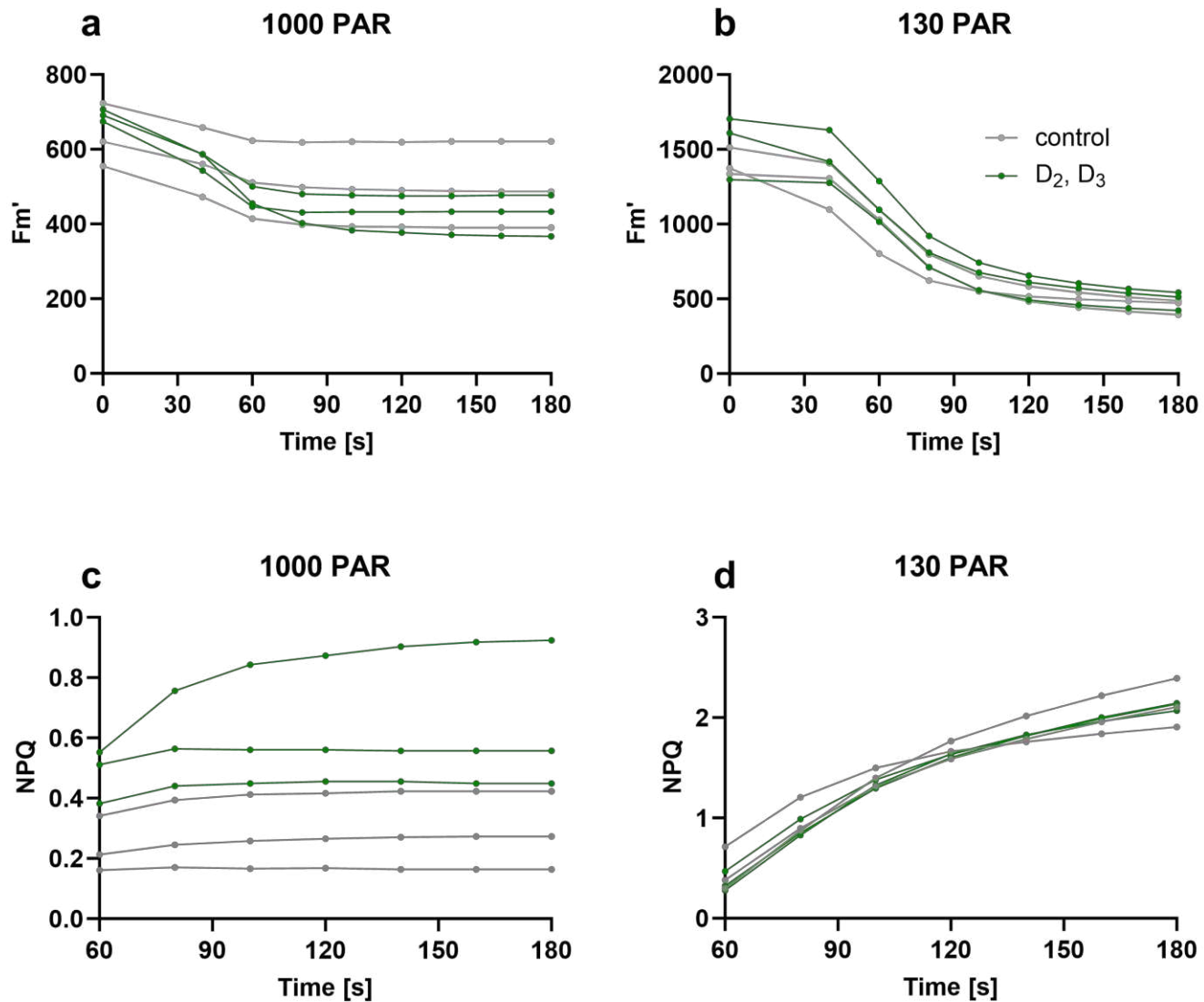


**Figure S4. Temporal dynamics in NPQ and Fm' values of vitamin D-treated algae, exposed to regular or excess light.** Temporal dynamics in Fm' and NPQ of both control and vitamin D-treated algae exposed to regular light levels (130 PAR) or excess light levels (1000 PAR) for 2 hours prior to analysis. The timing of saturating pulses is represented by dots. NPQ values were measurable from t=60s onwards. Each line represents a single biological replicate.

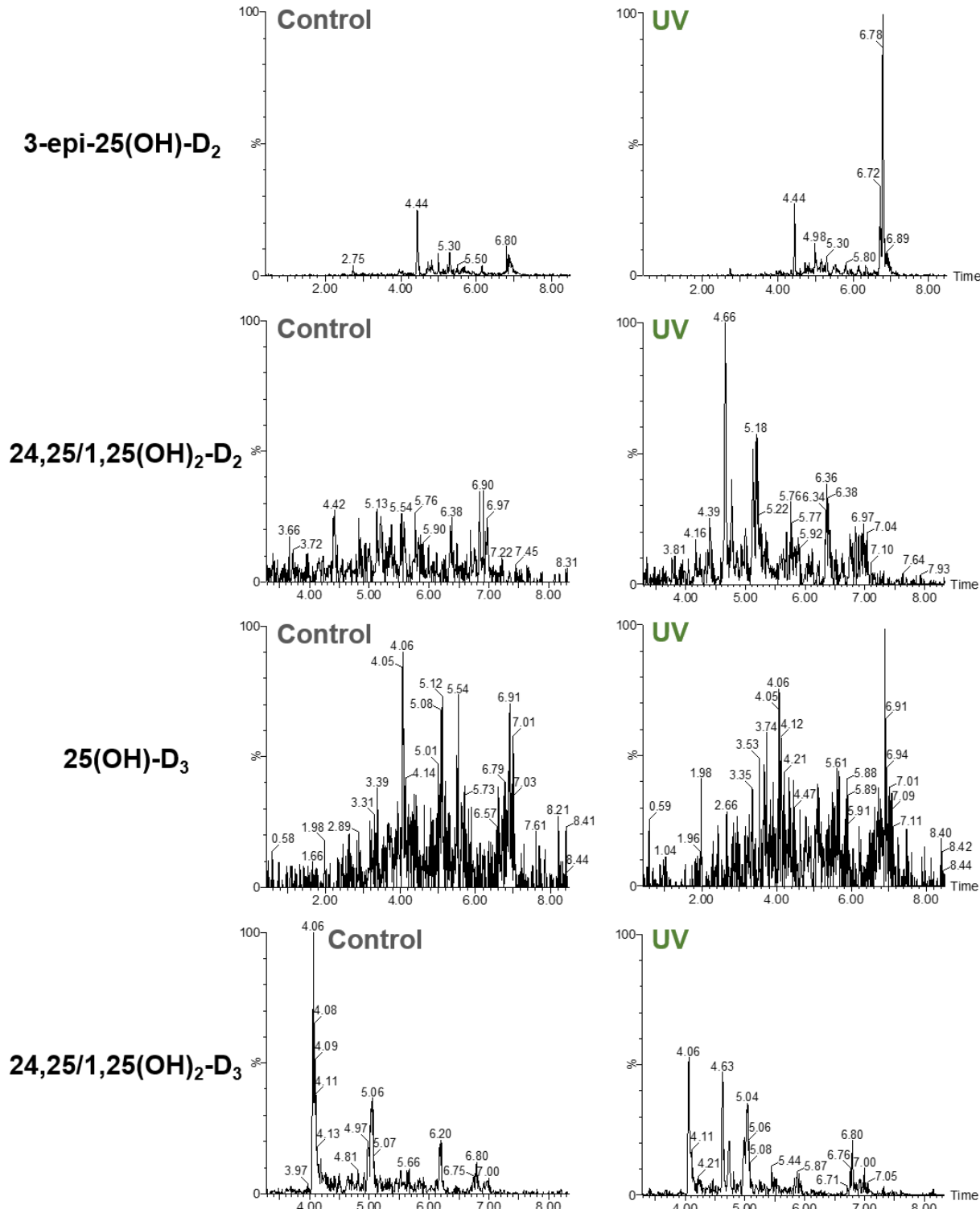


**Figure S5. *E. huxleyi* algae produce putative hydroxylated vitamin D species.** Representative chromatograms of hydroxylated vitamin D species detected in UV-treated and control cultures. The range of the Y axis in chromatograms of the same vitamin D species are identical and therefore comparable. The identification of metabolites is putative according to MRM taken from Oberson et al.<sup>77</sup>. Further analysis against standards is needed in order to verify the identification of the hydroxylated species.

681

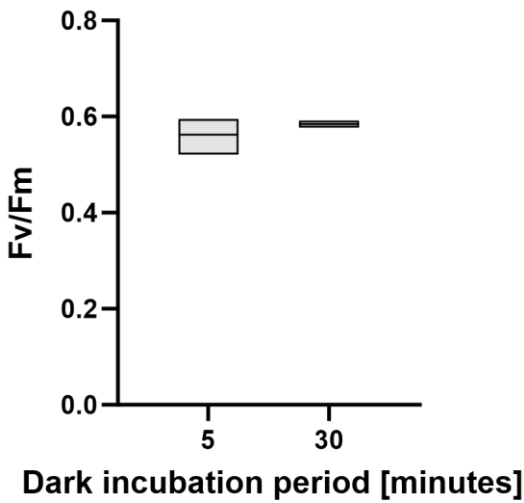


**Figure S6. Dark adaptation of 5 minutes sufficiently relaxes PSII reaction centers.** Comparison of maximum PSII quantum yields ( $F_v/F_m$ ) between algae that were dark-adapted for 5 or 30 minutes, calculated based on three biological replicates.

Gene	Forward	Reverse
G6284	GCCCTACCGGGTGTATCC	CTCGACTTGGTTGAGAACTTGC
G18115	CACCGAGCCGACCCAAAAT	TTCATCTCGGTCGTTGACAGG
G18590	CTCCTCGCGATGCAGAACAA	CCCTTCTGCCAACGTGATCT
G25467	TACGAGAACATGGCTGCTACG	CCCGTCGGACCTTAAGACAG
G12503	TCTCGGTGGAAATGGCGAC	ATTGTCATCGAGGCCGAAA
G93	GTCACGCCCGCGACAAA	GCGATGTGCGGGTGTATCT
G12340	AACCTGCTGCCGACATGAT	GGTTGAATCAGCATTGACCCC
G14992	GCGGGCTCTACTGAATCCG	GGGTCCCTCGTAGAAGGTGTG
G16746	TCGAAGATCCGGACGACGAT	AGCGCGAGACGAAAATAACG
G2511	TTGTCGCGTCGCTACTTT	GCCGAAGTAGTACGCCATGT
G2758	ATGGACCTAGACTCGGACGG	ACAGCCCTCAAGCTCACATC
G8907	CTCTCGTCTCGTGCTTCTT	TCGTAGATGTACTTGCCGGG
G26534	CTGGAAGATCGAGGCAACGG	TATGGCGTCGCCGTAAAG
G26797 <i>alpha-tubulin</i>	CGAGAAGGCGTACCAACGAG	CTTCGCTTGATGGTGGCGA
G28192 <i>beta-tubulin</i>	CAACATGAAGTGCGCCATCT	CCTCGGTGAACCTCCATCTCG
G1895 <i>rpl13</i>	ACCAGCACTTCCACAAGACG	TGCCGCAGCTTGTAGTTGTA

**Table S2. Primers used in this study.** Gene identifiers in *E. huxleyi* CCMP3266<sup>94</sup>. Primers were used to generate qRT-PCR data using *E. huxleyi* CCMP3266 cDNA.